Modelization of anaerobic processes during co-digestion of slowly biodegradable substrates

J.A. Rubio[1], J.L. Garcia-Morales[1], L.I. Romero[2] and F.J. Fernandez-Morales[3*]

[1] University of Cadiz, Environmental Technologies Department, Faculty of Marine and Environmental Sciences – Institute of Viticulture and Agri-Food Research (IVAGRO) – International Campus of Excellence (ceiA3), 11510 Puerto Real, Cádiz, Spain.

[2] University of Cadiz, Chemical Engineering and Food Technology Department, Faculty of Science – Institute of Viticulture and Agri-Food Research (IVAGRO) – International Campus of Excellence (ceiA3), 11510 Puerto Real, Cádiz, Spain.

[3]University of Castilla-La Mancha, ITQUIMA, Chemical Engineering Department, Avenida Camilo José Cela S/N. 13071, Ciudad Real, Spain.

* Corresponding author: Francisco Jesús Fernández Morales

University of Castilla-La Mancha, ITQUIMA, Chemical Engineering Dept., Avda. Camilo José Cela S/N 13071, Ciudad Real, Spain.

Tel: 0034 926 295300 (ext. 6350), Fax: 0034 926 295242.

E-mail: fcojesus.fmorales@uclm.es

Orcid iD: 0000-0003-0389-6247

Abstract

The influence of the soluble substrates over the anaerobic processes has been extensively investigated, but little is known about the effects of particulate substrate. The biodegradation of these substrates starts with the hydrolytic step, this process is slower than the other ones involved in the biodegradation of particulate substrates and usually becomes the rate-limiting step. This study investigate the effect of the initial total solids (TS) concentration on the anaerobic co-digestion of two slowly biodegradable organic substrates. The wastes mixtures were prepared at different dilutions in the range from 10% to 28% TS. From these experiments it was observed that as TS concentration increased, the methane production decreased. These results were modelled and it was observed that neither hydrolysis nor fermentation stages controlled the methane production rate. Being a substrate inhibition event experienced at the methanogenic stage the responsible of the lower methane production when operating at high TS concentrations.

Keywords: Anaerobic co-digestion; hydrolysis rate; inhibition; particulate substrate.

1. INTRODUCTION

The anaerobic co-digestion can be defined as the simultaneous biological treatment of two, or more biodegradable wastes. The combination of substrates with different compositions could be used to enhance the biogas production due to the equilibration of the nutrients balance in the mixture, mainly C/N ratio (Bohutskyi et al., 2018; Zahan et al., 2018), at the same time that the particulate substrates as well as toxic or inhibitory compounds concentrations could be diluted (Mata-Alvarez et al., 2000; Xie et al., 2016).

In the anaerobic digestion process, the presence of particulate substrates is relevant for the extension of the treatment due to the multiphase, multistage and sequential reactions required for its final transformation. The term hydrolysis define the breakdown of particulate substrates into biodegradable soluble substrates (Henze et al., 1987). Before its biodegradation, it is necessary to hydrolyse the particulate substrates (Levine et al., 1985). In most of the cases, the rate of hydrolysis is much slower than that of the consumption of the soluble substrates that it generates. Because of that, usually the hydrolysis stage became the rate limiting step in the biological treatment of the particulate pollutants (Henze et al., 1987). In the literature, it has been described that the hydrolytic processes play a dominant role in the delicate balance of electron donor/electron acceptor ratio of several bio-processes (Gujer and Zehnder, 1983; Levine et al., 1991; Rodríguez Mayor et al., 2004; de los Ángeles Fernandez et al., 2016). In the literature, different experimental approaches have been used to evaluate the anaerobic hydrolysis process. Some generalised approaches cannot be used for accurate estimation of the kinetic and stoichiometry of the anaerobic hydrolysis process. This is because the different populations/wastes involved in the study leads to large uncertainty (Morgenroth et al., 2002). In other cases, the studies of the hydrolysis involve the measurement of specific hydrolytic enzymes, intermediates or end-products (Brethauer et al., 2011). However, caution should be employed, when applying these results because slight changes in the wastes could

yield different results. Because of that, methods based on real effluents seems more convenient (Kouas et al., 2018).

Nowadays, the IWA Anaerobic Digestion Model No. 1 (ADM1) (Batstone et al., 2002) is one of the most widely used for anaerobic digestion modelling. This model accurately describes the stages taking place in the anaerobic digestion process, but presents a complex structure. Because of its complex structure, this model requires a detailed substrate characterization, which could be difficult to obtain, and the definition of the stoichiometric coefficients and kinetics rates of a wide number of processes (Goel et al., 1998). The large number of parameters make this model difficult to identify and may result in parameter correlation, leading to a significant uncertainties. Currently, several simplified anaerobic digestion models (Giovannini et al., 2018; Kouas et al., 2018; Kouas et al., 2019) adequately predict the process in most of the cases avoiding the complexity of the ADM1. However, when the wastes present components different to the conventional ones (Mata-Alvarez et al., 2000) or when the waste presents high solids contents, these simplified models present limitations in its accuracy (Morgenroth et al., 2002; Vavilin et al., 2008; Mao et al., 2019).

In this context, the aim of this work was to develop and validate a, mass balance based, simplified model describing the hydrolysis and subsequent processes in anaerobic co-digestion of two slowly biodegradable organic wastes, the 2POMW and the CM. The work pays special attention to the effects of the initial solids concentration, covering the wet as well as the dry anaerobic digestion, and to the hydrolytic stage on the operational evolution and biogas production.

2. MATERIALS AND METHODS

2.1 Experimental design

The experiments were designed to evaluate the hydrolytic as well was the subsequent processes of the anaerobic biodegradation of the solid wastes mixtures. Two organic wastes were used: two phase olive mill waste (2POMW) and Cattle manure (CM). 2POMW was collected from an olive oil mill (Cooperativa Nuestra Señora de los Remedios) located in Olvera, Cádiz (Spain). CM was obtained from a semi-intensive livestock farm located in El Puerto de Santa Maria Cádiz (Spain). Both substrates were homogenized and stored at -4ºC to preserve its original characteristics. The main physical–chemical characteristics of 2POMW and CM used in this study can be found in the supplementary material, Table S1.

On the one hand, the 2POMW is a by-product from oil olive extraction process in which a horizontal centrifuge is used to separate the oil fraction from this residue. This by-product was a semisolid waste, slightly acidic, presenting a high solid and organic matter content. The 2POMW contains compounds as lignin, hemicellulose, cellulose, fats, water-soluble carbohydrates and proteins (Morillo et al., 2009). Additionally, the 2POMW also presented a high C/N ratio (41.23) and a concentration of soluble phenolic compounds of 1,6 g L^{-1}. In the literature, it has been described that the presence of phenolic compounds in 2POMW depends on the fruit (type, maturity, etc.), climatic conditions and processing technique (Alburquerque et al., 2004; Morillo et al., 2009). The CM contains the faeces and urine from the animal, used bedding, sand and sediments (Cong et al., 2018). On the other hand, the CM was also characterized by a high organic nitrogen content, but presented low C/N ratio (18.52) and high pH values. A high proportion of the CM´s organic load correspond to cellulose, hemicelluloses and lignin (Bernal et al., 2009).

Previous studies demonstrated that the anaerobic digestion of 2POMW and CM yielded a maximum biogas production when mixed in a 75:25 ratio (2POMW:CM) (Pagés Díaz et al., 2011; Giuliano et al., 2013; Rubio et al., 2019). Based on these results, the mixtures used in this

study were prepared keeping the ratio 2POMW:CM constant but modifying the total solids percentage by diluting with demineralised water. Working in this way the reactors operated at a 10%, 15%, 20% and 28% of total solids (TS) percentage. The TS percentage were selected in order to cover the study of the performance of wet and dry anaerobic digestion. These tests were named, by their TS percentage, as R10, R15, R20 and R28.

2.2 Reactor set-up and operation

The anaerobic reactions were carried out in laboratory-scale batch anaerobic digesters of 2 L working volume and 1 L for the head space volume. A scheme of the reactor can be found in the supplementary material, Figure S1. These reactors were hermetically sealed to ensure anaerobic conditions during the digestion process, the wastes contained in the reactor were continuously mixed by means of a mechanical stirrer. These reactors were operated in the mesophilic range, at 35°C, and at a HRT of 15 d. The reactors were filled with the co-substrates mixture up to 80% of effective volume (1600 mL) and were completed with 400 mL of inoculum. These reactors were innoculated with a mesophilic seed from a laboratory digester acclimatised to the treatment of the 2POMW and CM. The main physical–chemical characteristics of the inoculum used in this study can be found in the supplementary material, Table S1. The digester had two ports for sampling and biogas output. Samples were taken three times a week and subsequently analysed. The biogas produced was collected in a 5 L Tedlar® bags for its subsequent analysis. The volumetric biogas production was quantified using a high precision gas meter (Ritter® Drum-type Gas Meter, 0.1 mbar). All the parameters determined were analysed in triplicate. In order to ensure similar initial pH values, the pH of all the mixtures were adjusted to 8.0 by adding a solution, 2.8 M, of Na_2CO_3.

2.3 Analytical techniques

The analytical parameters used for the physicochemical characterization of co-substrates and

monitoring the batch test were determined according to the Standard Methods (American Public Health Association, 2005). Total solids (TS), total volatile solids (VS), pH and total nitrogen Kjeldahl (TNK) were determined directly from the samples. Soluble chemical oxygen demand (COD_S), dissolved organic carbon (DOC), alkalinity, total phenols and volatile fatty acids (VFA) were measured over samples previously lixiviated. To do that, 10 g of sample were mixed with 100 mL of distilled water during 30 minutes. Then the mixture was filtered through a 0.45 µm glass-fibre filter. The DOC was determined by combustion/non-dispersive infrared gas analysis method using a total organic carbon analyser Shimadzu® TOC-5000 (Fernandez et al., 2008). Total phenols were determined by liquid chromatography according to the procedure described in the literature (Medina et al., 2011). The chromatographic system consisted of a Waters 717 plus autosampler, a Waters 600E pump, and a Waters 996 diode array detector (Waters Inc., Milford, MA). A Spherisorb ODS-2 (5µm, 25 cm X 4.6 mm i.d., Waters Inc.) column was used. Separation was achieved using an elution gradient with an initial composition of 90% water at pH 2.3 adjusted with phosphoric acid) and 10% methanol. The concentration of the methanol was increased to 30% over 10 min and maintained for 20 min. Subsequently, the methanol percentage was raised to 40% over 10 min, maintained for 5 min, and then increased to 50%. Finally, the methanol percentage was increased to 60%, 70%, and 100% in 5 min periods. A flow of 1 mL/min and a temperature of 35°C were used. Phenolic and oleosidic compounds were monitored at 280 and 240 nm, respectively. For determination of VFA, the following procedure was used: samples were lixiviated and then filtered through a 0.22 µm Teflon filter, acidified with a solution 1:2 (v/v) of phosphoric acid, spiked with phenol as internal standard and, finally, analysed in a gas chromatograph (Shimadzu® GC-2010) equipped with a flame ionization detector and using a capillary column filled with Nukol (polyethylene glycol modified by nitroterephthalic acid). The temperatures of the injection port and detector were 200 and 250 ºC, respectively. Hydrogen and synthetic air were used for the gas chromatograph flame ionization at 40 and 400 mL min^{-1}. Total acidity (TVFA) was

166 calculated by the addition of individual VFA levels, taking into account the molecular weights
167 of the different VFAs in order to express this parameter as acetic acid concentration.
168 The main components of biogas (hydrogen, methane and carbon dioxide) were determined by
169 gas chromatography (Shimadzu® GC-14 B) with a stainless steel column packed with Carbosive
170 SII and a thermal conductivity detector. The injected sample volume was 1 mL and the
171 operational conditions were as follows: 7 min at 55 ºC; followed with a ramp of 27ºC min^{-1} until
172 the temperatures reached 150 ºC; detector temperature: 255 ºC; injector temperature: 100ºC.
173 The carrier was helium and the flow rate used was 30 mL min^{-1} (Fdez-Güelfo et al., 2012).
174

175 ***2.4 Determination of non-solubilized carbon (NSC), Fermentable carbonous substrate (FCS)***
176 ***carbonous fermentation products (CFP).***

177 To evaluate the performance of the hydrolysis and the subsequent processes, as well as to
178 quantify the biodegradable fractions involved in each process, the trends of non-soluble carbon
179 (NSC), fermentable carbonous substrate (FCS) and carbonous fermentation products (CFP)
180 were determined. A scheme of the transformation is presented below.

181 $$NSC\ (p) \xrightarrow{Hydrolysis} \underbrace{FCS(s) \xrightarrow{Fermentation} CFP(s)}_{DOC}$$

182 The NSC is the particulate fraction of the organic carbon to be hydrolysed. The FCS is the
183 fraction of solubilized organic matter that has been transformed into fermentable substrates.
184 CFP represents the fraction of soluble organic carbon in acid form, i.e. the fraction
185 corresponding to VFAs. The sum of FCS and CFP fractions account to the Dissolved Organic
186 Carbon (DOC).
187 The NSC and FCS were determined according to equations (1) and (3) proposed in literature
188 (Fdez-Güelfo et al., 2012). The CFP was calculated according to equation (3) where AiH,
189 represents the concentration of each individual VFA measured by gas chromatography; ni, is
190 the number of carbon atoms of each AiH; MWi, is the molecular weight of each AiH. The total
191 organic carbon (TOC) was calculated from equation (2) as suggested by (Navarro et al., 1993).

$$NSC = TOC - DOC \quad (1)$$

$$TOC = VS \cdot 0.51 \quad (2)$$

$$CFP = \sum_{i=2}^{i=7} {AiH}/{MWi} \quad (3)$$

$$FCS = DOC - CFP \quad (4)$$

2.5 Model structure

The hydrolysis process sum up several steps such as lysis, non-enzymatic decay, phase separation, diffusion, adsorption, reaction, physical breakdown, etc. of particulate substrate (Vavilin et al., 2008). Because of that, the first order kinetics appears to be not applicable under all circumstances and therefore it is needed a model that accurately describe the disintegration and hydrolysis steps. In the literature, the Contois model has been demonstrated to adequately describe experimental data sets from a wide range of organic wastes (Sötemann et al., 2006; Nopharatana et al., 2007; Vavilin et al., 2008). The Contois model can be written as presented in equation (5):

$$\rho_{process} = k_{m,process} \cdot X \cdot \frac{S}{K_{S,process} \cdot X + S} = k_{m,process} \cdot X \cdot \frac{{S}/{X}}{K_{S,process} + {S}/{X}} \quad (5)$$

where $\rho_{process}$ is the process rate (g C kg^{-1} fresh weight d^{-1}); $k_{m,process}$ is the maximum specific uptake rate of the process (d^{-1}); $K_{S,process}$ is the half-saturation coefficient for the ratio S/X (g C kg^{-1} fresh weight); X is the hydrolytic (disintegration) biomass concentration (g C kg^{-1} fresh weight) and S is the particulate compound concentration (g C kg^{-1} fresh weight).

The fermentative and the methanogenic stages can be described by Monod Kinetics (Jeong et al., 2005; Fernandez-Morales et al., 2010; García-Gen et al., 2013). In addition, the anaerobic biodegradation of 2POMW produces a large quantity of polyphenols which could cause inhibition (Rubio et al., 2019). This inhibition event is usually observed by a decrease of the methane production and an accumulation of VFAs (Chen et al., 2008; Zhang et al., 2019). This phenomenon can be explained by the relationship between the polypohenols and the

propionic generation (Morillo et al., 2009) which leads to an inhibition in the methanogenic stage. Because of that, a non-competitive function was included for modelling the inhibition in the methanogenic stage according to the Hill function (Hill and Barth, 1977) this function is presented in equation 6:

$$I_P = b \cdot \left[1 - \frac{S_P}{K \cdot S_P + S_{P,lim}}\right] \quad (6)$$

where IP is propionic inhibition factor of acetoclastic methanogens, S_P is the propionic concentration (g C kg^{-1} fresh weight), $S_{P,lim}$ is the mean propionic threshold concentration (g C kg^{-1} fresh weight), K is the Hill coefficient which defines the slope of the drop in the inhibition function.

The processes rates and stoichiometry of the developed model is presented in Table 1 as a Petersen matrix.

228 **Table 1.** Petersen matrix of the main anaerobic degradation processes taking place during the co-digestion of POMW and CM.
229

Component									
Process	**NSC**	**FCS**	**CFP**	**CH_4**	**CO_2**	**Xh**	**Xf**	**X_{CH4}**	**Process rate**
Hydrolysis	-1	(1-Yh)				Yh			$kh \cdot \frac{NSC/_{Xh}}{K_{s,h} + NSC/_{Xh}} \cdot Xh$
Fermentation		-1	(1-Yf)				Yf		$kf \cdot \frac{FCS}{K_{s,f} + FCS} \cdot Xf$
Methanogenesis			-1	$(1-Y_{CH4}) \cdot f_{CH4}$	$(1-Y_{CH4}) \cdot f_{CO2}$			Y_{CH4}	$k_m \cdot \frac{CFP}{K_{s,m} + CFP} \cdot X_m \cdot \left[1 - \frac{S_P}{K \cdot S_P + S_{P,lim}}\right]$
Decay Xh	1					-1			$k_{dec,Xh} \cdot Xh$
Decay Xf	1						-1		$k_{dec,Xf} \cdot Xf$
Decay X_m	1							-1	$k_{dec,Xm} \cdot X_m$
Nomenclature	*Yh: Yield of biomass on the hydrolysis process* *Yf: Yield of biomass on the fermentation process* *Y_{CH4}: Yield of biomass on the methanogenic process* *f_{CH4}: Yield, catabolism only, of methane* *f_{CO2}: Yield, catabolism only, of carbon dioxide* *kh: Hydrolysis rate* *kf: Fermentation rate* *km: Methanogenesis rate*					*ks,h: Half saturation constant of the substrate in the hydrolytic process* *ks,f: Half saturation constant of the substrate in the fermentation process* *ks,m: Half saturation constant of the substrate in the methanogenic process* *Xh: Hydrolytic biomass* *Xf: Fermentative biomass* *Xm: Methanogenic biomass* *$k_{dec,Xh}$: Hydrolytic biomass decay rate* *$k_{dec,Xf}$: Fermentative biomass decay rate* *$k_{dec,Xm}$: Methanogenic biomass decay rate*				

3. RESULTS AND DISCUSSION

The increased in the TS concentration leads to an increase in the organic substrates available in the system. This increase in the substrate available for the microbial metabolisms could lead to a higher biogas production or to a lower one because of inhibitory effects in the different stages involved in the anaerobic digestion. In order to study the performance of the anaerobic digestion, several experiments were carried out and modelled. Before the modelling, the mass balance reconciliation was checked, obtaining a reconciliation higher than 90% in all the cases.

3.1 Assessment of biomass fractions

The modelization of the experimental results requires the determination of the substrate fractions involved in the processes modelled. In this work, the characterization of the substrate mixtures was carried out following the procedure previously described in the literature (Navarro et al., 1993; Fdez-Güelfo et al., 2012) and the results obtained are presented in Table 2.

Table 2. Carbon fractions in the wastes mixture.

% TS	NSC (g kg^{-1} fresh weight)	FCS (g kg^{-1} fresh weight)	CFP (g kg^{-1} fresh weight)
10	25.6	9.60	0.15
15	34.5	13.62	0.20
20	55.5	17.99	0.33
28.6	73.3	27.00	0.22

From the characterization of the mixtures, it can be seen the very high NSC fraction, which accounted to about a 73% of the total carbon contained in the mixtures. This particulate fraction is the fraction that could be hydrolysed to form FCS. At the beginning of the tests, the FCS concentration was about 27%. Finally, the smallest fraction was the CFP, which accounted in all the cases percentages lower than 5% of the carbon concentration. The very low CFP

concentration could be explained because of its very high biodegradability which leads to a fast consumption when it is generated (de Lucas et al., 2007).

3.2. Reactor operation

As stated above, the source of substrate fed to the reactors was the same in all the cases, being the only difference its initial TS concentration which ranged from 10 to 28%. Because of that, the different performances observed could only be explained because of the different initials TS concentrations. In Figure 1 it is presented the evolution of the NSC fraction along the experiments. As can be seen in this Figure, the NSC fraction reached the steady-state conditions after about 80 d.

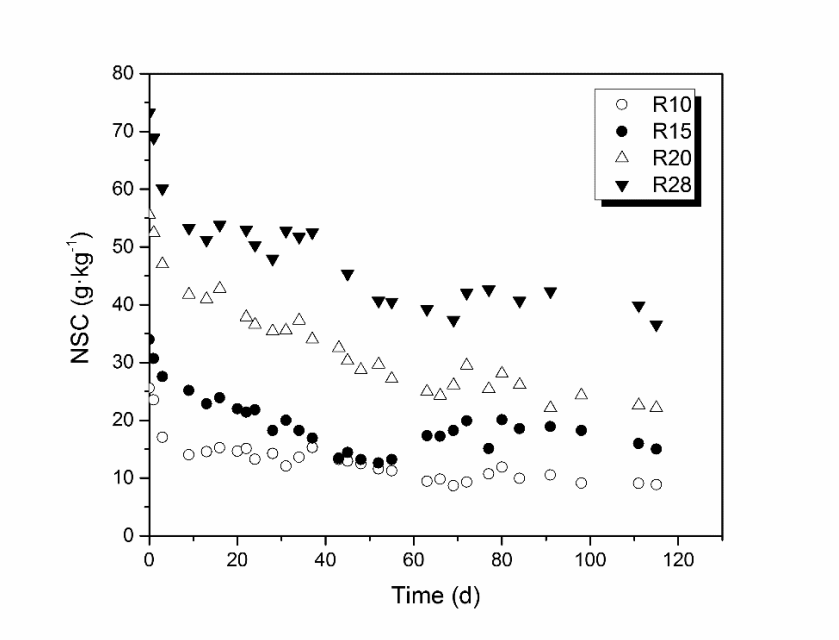

Figure 1. Evolution of the NSC fraction during the co-digestion of 2POMW and CM.

The increasing remanent NSC with the increasing initial concentration, could be related to the accumulation of hardly hydrolysable compounds in the reactors quantified within the NSC

fraction or due to inhibitory events. In this work, the almost constant percentage of the NSC removal in all the cases, about 55%, ratified the accumulation of hardly hydrolysable compounds. Moreover, the final concentration of the NSC fraction accounted about 75% of total organic carbon (TOC) in the reactors. According to the literature, this value corresponds to the insoluble lignocellulosic fractions of the wastes used (Alburquerque et al., 2004). These saccharide chains are connected by hydrogen bonds and aggregated to form a three dimensional structure of fibrils, which are characterised by its toughness and water insolubility (Wang et al., 2020). A similar behaviour was observed when removing the FCS fraction, results not shown. In this case the non-fermentable fraction was also in all the cases almost the same, about a 50%.

Regarding to the biogas production, it must be highlighted the existence of a lag phase when dealing with high TS concentrations. Table 3 shows the most relevant information related to the biogas production in the different reactors.

Table 3. Main parameters in the methanogenic stage.

	Units	R10	R15	R20	R28
Lag phase length	d	10	16	22	34
Methane yield	g C kg^{-1} fresh weight	5.3	4.8	1.2	1.0
Methane composition	CH_4:CO_2	80:20	75:25	70:30	65:35
Methane selectivity	g C g^{-1} C consumed	0.80	0.76	0.71	0.64

As can be seen in Table 3, the length of the lag phase linearly increased when the TS concentration increases. In the literature, the length of the lag phase has been related to different operational parameters. Such as inoculum size, physical conditions, inhibitors presence, etc. (Tsao, 1976; Baranyi and Roberts, 1994). Taking into account that in this work

288 the inoculum was the same in all the cases, the variation in the lag phase length only can be
289 caused by the different initial TS concentrations experienced.
290 When comparing the methane yield, it was observed that it decreased as the initial NSC
291 concentrations increases. This event only could be explained by an inhibition effect when
292 operating at higher TS percentages. It is also remarkable that the higher the TS percentages
293 the lower the CH_4:CO_2 in the biogas obtained, presenting a linear trend with an intercept of 5
294 and a slope of -0.1 (R^2= 0.93). The explanation can be found in the two pathways of methane
295 generation, the hydrogenotrophic and the acetoclastic. At the beginning of the processes, the
296 methane was generated mainly by hydrogenotrophic activity, which is characterised by ratios
297 CH_4:CO_2 lower than 2 (Montero et al., 2008). This point was confirmed by the negligible
298 concentrations of hydrogen and the absence of VFAs degradation observed at the beginning of
299 the processes in spite of the initial TS concentration, see Figure S2. After that, the acetoclastic
300 culture could have been developed increasing the methane percentage in the biogas.
301 However, the development of the acetoclastic culture could have been not significant when
302 operating at high TS concentrations. In the literature, it has been described a higher proportion
303 of hydrogenotrophic methanogens in reactors operating with high TS content (Montero et al.,
304 2008). Then, the operation with high TS content in the anaerobic reactors leads to a longer lag
305 phase and to a prevalence of the hydrogenotrophic methanogenic culture which generated
306 biogas with lower methane percentages.
307 With the aim to deep into the mechanisms of the anaerobic transformations taking place
308 during the anaerobic digestion of the wastes studied, the methane selectivity was calculated as
309 the ratio of the methane-carbon generated to the total amount of carbon consumed in the
310 process, the obtained results are presented in Table 3. As can be seen in this Table, the higher
311 the TS percentage, the lower the methane yield and selectivity. These results indicates that a

312 controlling stage or an inhibition event affected the methanogenic reaction (Li et al., 2019; Shi
313 et al., 2019). In order to identify in which stage the inhibition took place, modelling works of
314 the hydrolysis, fermentation and the methanogenic stage were performed by using the model
315 previously described.
316
317 ***3.3. Model calibration and validation***
318 The model previously described was calibrated to fit the experimental data set obtained in the
319 co-digestion experiments with 10%, 15% and 28% of TS. As example, the calibration when
320 treating a 10% mixture is presented in Figure 2.
321
322 a)

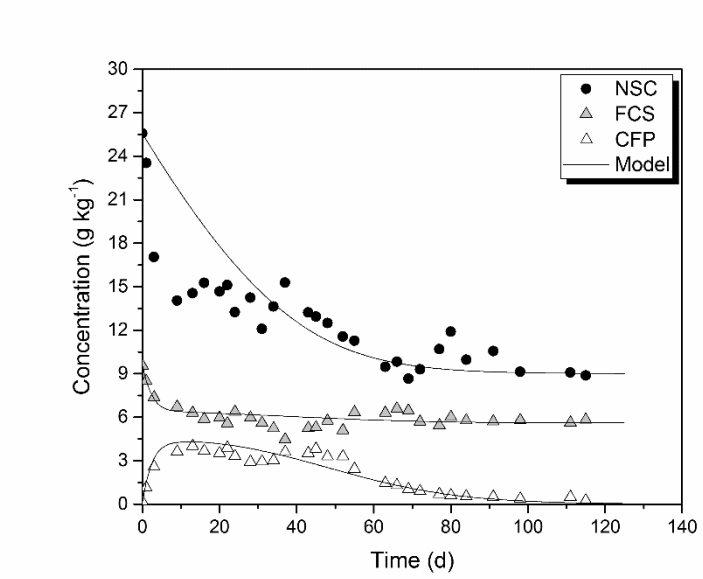

323
324
325
326
327

b)

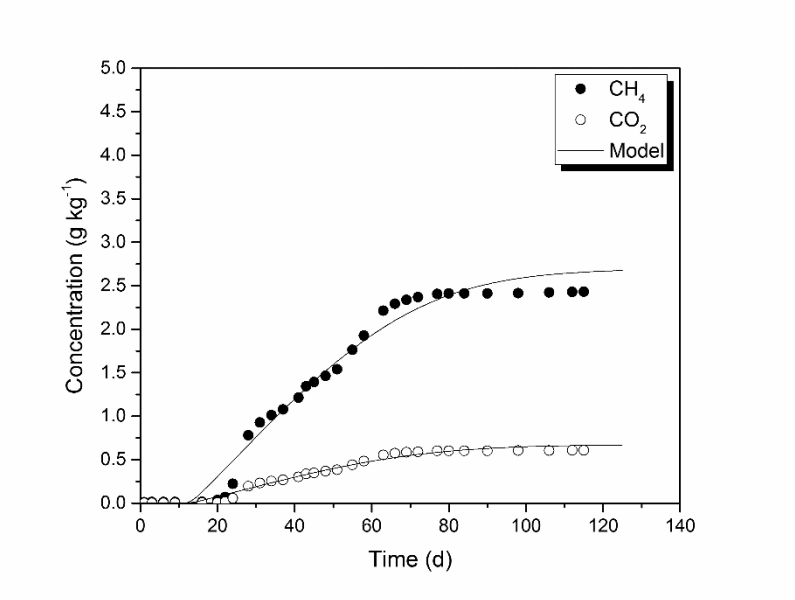

Figure 2. a) Results of the model calibration of carbon fractions and b) biogas evolution with experimental results of the co-digestion at 10% TS.

As can be seen in Figure 2, the calibrated model accurately described the performance of the system when dealing with a TS concentrations of 10%. A similar accuracy was obtained in the other concentrations studied, 15 and 28%, in spite of the different initial TS concentrations. The values of the main kinetic and stoichiometric parameters obtained after the calibration of the model are presented in Table 4. The parameter not presented in Table 4 were fitted with the typical values indicated in the literature (Batstone et al., 2002).

Table 4. Main kinetic and stoichiometric parameters of the model.

% ST	NSC		FCS		CFP			
	kh (d^{-1})	*Ks* (g C kg^{-1})	*kf* (d^{-1})	*Ks* (g C kg^{-1})	*km* (d^{-1})	*Ks* (g C kg^{-1})	*K*	C_{Lim} (g C kg^{-1})
10.0	0.70	10	2.50	4.0	0.75	4.0	0.95	2.7
15.0	0.69	10	2.47	4.0	0.76	4.0	0.90	2.6
28.6	0.70	10	2.50	4.0	0.75	4.0	0.99	2.7
Calibration value	**0.70**	**10**	**2.49**	**4.0**	**0.75**	**4.0**	**0.95**	**2.7**
Standard deviation	**0.01**	**0**	**0.02**	**0**	**0.01**	**0.0**	**0.05**	**0.06**

The maximum specific rates were so strongly associated with the biomass concentration that the values could not be estimated individually. As can be seen in Table 4, the fitting values of the kh and kf were the same in all the cases. The consistent values of the kh and kf parameters indicates the absence of any inhibition or limitation in both, the hydrolytic and the fermentative processes. Theoretically, the mixture R28 could experience mass transfer limitations due to its very high TS concentration, within the range of the dry anaerobic digestion (Ten Brummeler et al., 1991). However, this limitations do not occur, which could be explained because it was easily hydrolysable and because of the particle size. It is known that small particle size presents high surface to volume ratio, making easier the hydrolysis and subsequent transformations.

With regard to the km values, they were the similar in all the cases, indicating that the maximum methanogenic rate is the same in spite of the initial TS concentration. However, this rate was modified by an inhibition expression. The data sets corresponding to the three series of experiments were simultaneously fitted, obtaining different lag phase lengths. The length of these lag phase were linearly proportional to the initial TS concentration. Additionally, the inhibition parameters were also very similar in all the cases, 0.95 for the K parameter and 2.7 for the threshold concentration, $S_{p,Lim}$. This inhibitory effect could be caused by the very high

363 concentration of VFA reached in the liquid bulk, see supplementary material Fig S2. This very
364 high VFA concentration can be explained because of the presence of polyphenols, which leads
365 to a very high propionic acid concentration (Pullammanappallil et al., 2001). When the
366 propionic acid concentration reached values higher than 2.7 g C kg^{-1} inhibition effects were
367 observed, see figure S2. The explanation this event could be explained because of the
368 dissociated form of the acid can pass across the cellular membrane (Castro-Villalobos et al.,
369 2012). Once inside the cell, a high maintenance energy consumption is required which could
370 inhibit, and even stop, the methanogenic reaction.
371 Once finished the calibration stage, the model was validated using the calibrated parameters
372 previously obtained. The experimental results as well as the predictions of the model obtained
373 during the validation with experimental data corresponding to the 20% TS concentration are
374 presented in Figure 3. As can be observed in these figures an accurate prediction was
375 obtained.
376
377 a)

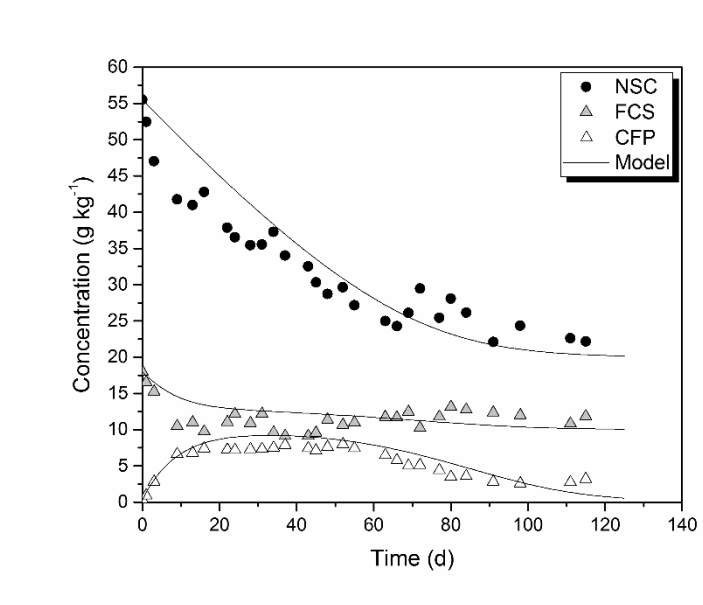

378

379 b)

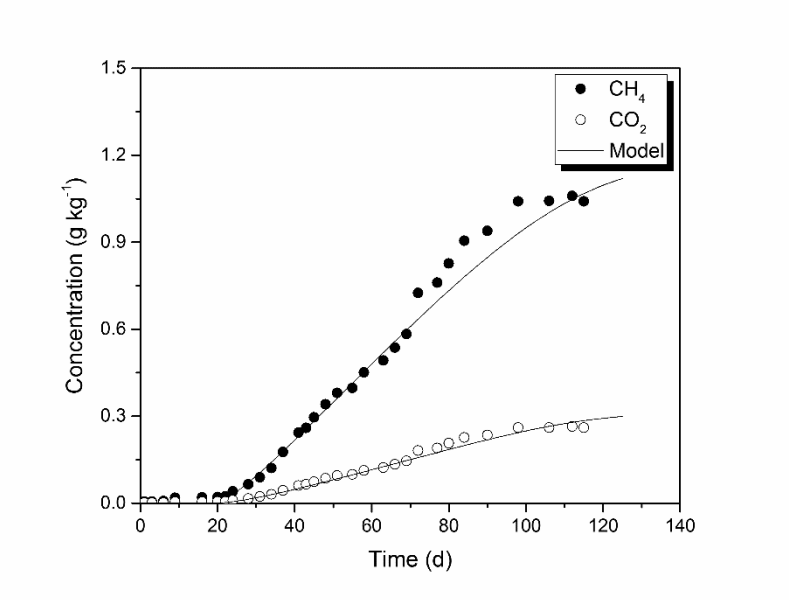

380

381 **Figure 3.** a) Validation of COD fractions and b) methane evolution with experimental results of
382 the co-digestion at 20% TS.

383

384 From the results obtained, it can highlighted that the hydrolysis and fermentation rates
385 obtained during the calibration accurately predicted the results obtained when co-digesting
386 the mixture with a 20% TS. This results indicates that, in spite of the very different initial TS
387 concentrations studied in this work, no limitations were observed in the hydrolysis and
388 fermentation rates. However, inhibition events were observed during the methanogenic stage.
389 The inhibition could be caused by the accumulation of fermentation products, mainly
390 propionic acid, which could be caused by the presence of polyphenols in the mixture. The
391 phenolic compounds are characteristic of the by-products from the olive oil extraction and
392 contains a benzene ring conjugated to a propionic acid. In the literature it has been described
393 that propionic acid from phenolic compounds can slow the anaerobic acetoclastic
394 methanogenesis (Palatsi et al., 2011) (Borja et al., 1997).

Conclusions

The fractionated disintegration of the substrates provided accurate information for the description of the co-digestion experiments. Additionally, the model developed allowed to accurately predict a wide spectrum of initial TS concentrations. From the modelling results, it was observed that the lower transformation rate was observed in the hydrolysis stage 0.7 d^{-1}. However, when operating at high TS concentrations the inhibition event experienced in the methanogenic stage slow down its rate becoming the controlling stage of the stabilization process. This inhibition event was caused by the propionic acid and described by a Hill inhibition function.

ACKNOWLEDGMENTS

The authors wish to express their gratitude to the Spanish Ministry of Science and Innovation, the European Regional Development Fund (ERDF) and the Junta de Andalucía, specifically to PROBIOGAS Project PS-120000-2007-6 and for providing financial support. The authors would also like to thank the collaboration of the olive mill facility ‘‘Nuestra Señora de los Remedios’’ in this project and the kind contribution of Dra. Concepción Romero Barranco in the analytical determination of polyphenols carried out at the Instituto de la Grasa (CSIC-Spain).

REFERENCES

Alburquerque, J.A., Gonzálvez, J., García, D., Cegarra, J., 2004. Agrochemical characterisation of "alperujo", a solid by-product of the two-phase centrifugation method for olive oil extraction. Bioresource Technology 91, 195-200.

American Public Health Association, E.A.D.A.W.W.A.W.E.F., 2005. Standard methods for the examination of water and wastewater. APHA-AWWA-WEF, Washington, D.C.

Baranyi, J., Roberts, T.A., 1994. A dynamic approach to predicting bacterial growth in food. International Journal of Food Microbiology 23, 277-294.

Batstone, D.J., Keller, J., Angelidaki, I., Kalyuzhnyi, S.V., Pavlostathis, S.G., Rozzi, A., Sanders, W.T.M., Siegrist, H., Vavilin, V.A., 2002. The IWA Anaerobic Digestion Model No 1 (ADM1). Water Science and Technology 45, 65-73.

Bernal, M.P., Alburquerque, J.A., Moral, R., 2009. Composting of animal manures and chemical criteria for compost maturity assessment. A review. Bioresource Technology 100, 5444-5453.

Bohutskyi, P., Phan, D., Kopachevsky, A.M., Chow, S., Bouwer, E.J., Betenbaugh, M.J., 2018. Synergistic co-digestion of wastewater grown algae-bacteria polyculture biomass and cellulose to optimize carbon-to-nitrogen ratio and application of kinetic models to predict anaerobic digestion energy balance. Bioresource Technology 269, 210-220.

Borja, R., Alba, J., Banks, C.J., 1997. Impact of the main phenolic compounds of olive mill wastewater (OMW) on the kinetics of acetoclastic methanogenesis. Process Biochemistry 32, 121-133.

Brethauer, S., Studer, M.H., Yang, B., Wyman, C.E., 2011. The effect of bovine serum albumin on batch and continuous enzymatic cellulose hydrolysis mixed by stirring or shaking. Bioresource Technology 102, 6295-6298.

Castro-Villalobos, M.C., García-Morales, J.L., Fernández, F.J., 2012. By-products inhibition effects on bio-hydrogen production. International Journal of Hydrogen Energy 37, 7077-7083.

Chen, Y., Cheng, J.J., Creamer, K.S., 2008. Inhibition of anaerobic digestion process: A review. Bioresource Technology 99, 4044-4064.

Cong, W.F., Moset, V., Feng, L., Møller, H.B., Eriksen, J., 2018. Anaerobic co-digestion of grass and forbs – Influence of cattle manure or grass based inoculum. Biomass and Bioenergy 119, 90-96.

de los Ángeles Fernandez, M., de los Ángeles Sanromán, M., Marks, S., Makinia, J., Gonzalez del Campo, A., Rodrigo, M., Fernandez, F.J., 2016. A grey box model of glucose fermentation and syntrophic oxidation in microbial fuel cells. Bioresource Technology 200, 396-404.

de Lucas, A., Rodriguez, L., Villasenor, J., Fernandez, F.J., 2007. Fermentation of agro-food wastewaters by activated sludge. Water Research 41, 1635-1644.

Fdez-Güelfo, L.A., Álvarez-Gallego, C., Sales, D., Romero, L.I., 2012. New indirect parameters for interpreting a destabilization episode in an anaerobic reactor. Chemical Engineering Journal 180, 32-38.

Fernandez, F.J., Sanchez-Arias, V., Villasenor, J., Rodriguez, L., 2008. Evaluation of carbon degradation during co-composting of exhausted grape marc with different biowastes. Chemosphere 73, 670-677.

Fernandez-Morales, F.J., Villasenor, J., Infantes, D., 2010. Modeling and monitoring of the acclimatization of conventional activated sludge to a biohydrogen producing culture by biokinetic control. International Journal of Hydrogen Energy 35, 10927-10933.

García-Gen, S., Lema, J.M., Rodríguez, J., 2013. Generalised modelling approach for anaerobic co-digestion of fermentable substrates. Bioresource Technology 147, 525-533.

Giovannini, G., Sbarciog, M., Steyer, J.P., Chamy, R., Wouwer, A.V., 2018. On the derivation of a simple dynamic-model of anaerobic digestion including the evolution of hydrogen. Water Research 134, 209-225.

Giuliano, A., Bolzonella, D., Pavan, P., Cavinato, C., Cecchi, F., 2013. Co-digestion of livestock effluents, energy crops and agro-waste: Feeding and process optimization in mesophilic and thermophilic conditions. Bioresource Technology 128, 612-618.
Goel, R., Mino, T., Satoh, H., Matsuo, T., 1998. Comparison of hydrolytic enzyme systems in pure culture and activated sludge under different electron acceptor conditions. Water Science and Technology 37, 335-343.
Gujer, W., Zehnder, A.J.B., 1983. Conversion processes in anaerobic digestion. Water Science and Technology 15, 127-167.
Henze, M., Grady Jr, C.P.L., Gujer, W., Marais, G.V.R., Matsuo, T., 1987. A general model for single-sludge wastewater treatment systems. Water Research 21, 505-515.
Hill, D.T., Barth, C.L., 1977. A dynamic model for simulation of animal waste digestion. Journal of the Water Pollution Control Federation 49, 2129-2143.
Jeong, H.-S., Suh, C.-W., Lim, J.-L., Lee, S.-H., Shin, H.-S., 2005. Analysis and application of ADM1 for anaerobic methane production. Bioprocess and Biosystems Engineering 27, 81-89.
Kouas, M., Torrijos, M., Schmitz, S., Sousbie, P., Sayadi, S., Harmand, J., 2018. Co-digestion of solid waste: Towards a simple model to predict methane production. Bioresource Technology 254, 40-49.
Kouas, M., Torrijos, M., Sousbie, P., Harmand, J., Sayadi, S., 2019. Modeling the anaerobic co-digestion of solid waste: From batch to semi-continuous simulation. Bioresource Technology 274, 33-42.
Levine, A.D., Tchobanoglous, G., Asano, T., 1985. Characterization of the size distribution of contaminants in wastewater: treatment and reuse implications. Journal of the Water Pollution Control Federation 57, 805-816 + 298a.
Levine, A.D., Tchobanoglous, G., Asano, T., 1991. Size distributions of particulate contaminants in wastewater and their impact on treatability. Water Research 25, 911-922.
Li, X.N., Yang, Z.Y., Liu, G.Q., Ma, Z.H., Wang, W., 2019. Modified anaerobic digestion model No.1 (ADM1) for modeling anaerobic digestion process at different ammonium concentrations. Water Environment Research 91, 700-714.
Mao, C., Xi, J., Feng, Y., Wang, X., Ren, G., 2019. Biogas production and synergistic correlations of systematic parameters during batch anaerobic digestion of corn straw. Renewable Energy 132, 1271-1279.
Mata-Alvarez, J., Macé, S., Llabrés, P., 2000. Anaerobic digestion of organic solid wastes. An overview of research achievements and perspectives. Bioresource Technology 74, 3-16.
Medina, E., Romero, C., de los Santos, B., de Castro, A., Garcia, A., Romero, F., Brenes, M., 2011. Antimicrobial Activity of Olive Solutions from Stored Alpeorujo against Plant Pathogenic Microorganisms. Journal of Agricultural and Food Chemistry 59, 6927-6932.
Montero, B., Garcia-Morales, J.L., Sales, D., Solera, R., 2008. Evolution of microorganisms in thermophilic-dry anaerobic digestion. Bioresource Technology 99, 3233-3243.
Morgenroth, E., Kommedal, R., Harremoës, P., 2002. Processes and modeling of hydrolysis of particulate organic matter in aerobic wastewater treatment - A review. Water Science and Technology, pp. 25-40.
Morillo, J.A., Antizar-Ladislao, B., Monteoliva-Sánchez, M., Ramos-Cormenzana, A., Russell, N.J., 2009. Bioremediation and biovalorisation of olive-mill wastes. Applied Microbiology and Biotechnology 82, 25-39.
Navarro, A.F., Cegarra, J., Roig, A., Garcia, D., 1993. Relationships between organic matter and carbon contents of organic wastes. Bioresource Technology 44, 203-207.
Nopharatana, A., Pullammanappallil, P.C., Clarke, W.P., 2007. Kinetics and dynamic modelling of batch anaerobic digestion of municipal solid waste in a stirred reactor. Waste Management 27, 595-603.

Pagés Díaz, J., Pereda Reyes, I., Lundin, M., Sárvári Horváth, I., 2011. Co-digestion of different waste mixtures from agro-industrial activities: Kinetic evaluation and synergetic effects. Bioresource Technology 102, 10834-10840.
Palatsi, J., Viñas, M., Guivernau, M., Fernandez, B., Flotats, X., 2011. Anaerobic digestion of slaughterhouse waste: Main process limitations and microbial community interactions. Bioresource Technology 102, 2219-2227.
Pullammanappallil, P.C., Chynoweth, D.P., Lyberatos, G., Svoronos, S.A., 2001. Stable performance of anaerobic digestion in the presence of a high concentration of propionic acid. Bioresource Technology 78, 165-169.
Rodríguez Mayor, L., Villaseñor Camacho, J., Fernández Morales, F.J., 2004. Operational optimisation of pilot scale biological nutrient removal at the Ciudad Real (Spain) domestic wastewater treatment plant. Water, Air, Soil Pollut. 152, 279-296.
Rubio, J.A., Romero, L.I., Wilkie, A.C., Garcia-Morales, J.L., 2019. Mesophilic Anaerobic Co-digestion of Olive-Mill Waste With Cattle Manure: Effects of Mixture Ratio. Frontiers in Sustainable Food Systems 3.
Shi, E., Li, J.Z., Zhang, M., 2019. Application of IWA Anaerobic Digestion Model No. 1 to simulate butyric acid, propionic acid, mixed acid, and ethanol type fermentative systems using a variable acidogenic stoichiometric approach. Water Research 161, 242-250.
Sötemann, S.W., van Rensburg, P., Ristow, N.E., Wentzel, M.C., Loewenthal, R.E., Ekama, G.A., 2006. Integrated chemical, physical and biological processes modelling of anaerobic digestion of sewage sludge. Water Science and Technology, pp. 109-117.
Ten Brummeler, E., Horbach, H.C.J.M., Koster, I.W., 1991. Dry anaerobic batch digestion of the organic fraction of municipal solid waste. Journal of Chemical Technology and Biotechnology 50, 191-209.
Tsao, G.T., 1976. Principles of microbe and cell cultivation, S. John Pirt, Halsted Press, Division of John Wiley and Sons, New York, 274 pages, $34.00. AIChE Journal 22, 621-621.
Vavilin, V.A., Fernandez, B., Palatsi, J., Flotats, X., 2008. Hydrolysis kinetics in anaerobic degradation of particulate organic material: An overview. Waste Management 28, 939-951.
Wang, X.Z., Yuan, T., Guo, Z.T., Han, H.L., Lei, Z.F., Shimizu, K., Zhang, Z.Y., Lee, D.J., 2020. Enhanced hydrolysis and acidification of cellulose at high loading for methane production via anaerobic digestion supplemented with high mobility nanobubble water. Bioresource Technology 297.
Xie, S.H., Hai, F.I., Zhan, X.M., Guo, W.S., Ngo, H.H., Price, W.E., Nghiem, L.D., 2016. Anaerobic co-digestion: A critical review of mathematical modelling for performance optimization. Bioresource Technology 222, 498-512.
Zahan, Z., Georgiou, S., Muster, T.H., Othman, M.Z., 2018. Semi-continuous anaerobic co-digestion of chicken litter with agricultural and food wastes: A case study on the effect of carbon/nitrogen ratio, substrates mixing ratio and organic loading. Bioresource Technology 270, 245-254.
Zhang, R., Anderson, E., Chen, P., Addy, M., Cheng, Y., Wang, L., Liu, Y., Ruan, R., 2019. Intermittent-vacuum assisted thermophilic co-digestion of corn stover and liquid swine manure: Salinity inhibition. Bioresource Technology 271, 16-23.